Atmospheric Environment 333 (2024) 120656

Contents lists available at ScienceDirect

Atmospheric Environment

journal homepage: www.elsevier.com/locate/atmosenv

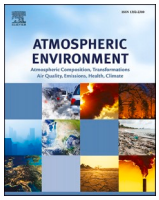

Characterization of aerosol and its oxidative potential in a coastal semi-rural site of Southern Italy

A. Dinoi [a], G. Pavese [b], M. Calvello [b], D. Chirizzi [c], A. Pennetta [a,d], G.E. De Benedetto [d], F. Esposito [e], C. Mapelli [a,*], D. Contini [a]

[a] Institute of Atmospheric Sciences and Climate - ISAC-CNR, Lecce, 73100, Italy
[b] Institute of Methodologies for Environmental Analysis - IMAA-CNR, Tito Scalo (Pz), 85050, Italy
[c] Experimental Zooprophylactic Institute of Puglia and Basilicata - IZSPB, Foggia, 71121, Italy
[d] Department of Cultural Heritage, University of Salento, 73100, Lecce, Italy
[e] University of Basilicata, School of Engineering, C. da Macchia Romana, 85100, Potenza, Italy

HIGHLIGHTS

- A campaign was conducted in a rural site of the Mediterranean area, affected by traffic emissions and biomass combustion.
- Mean OP_{DTTv} values were as high as those observed in suburban areas.
- Combustion sources were the major contributors to OP activity of $PM_{2.5}$.

ARTICLE INFO

Keywords:
$PM_{2.5}$
Carbonaceous fraction
Chemical composition
Oxidative potential

ABSTRACT

Considering the scarce number of studies investigating the oxidative potential of $PM_{2.5}$ in Italy, a measurement campaign was conducted from February 2020 to October 2020 in a coastal semi-rural site of Basilicata (Southern Italy) with the goal to characterize the fine fraction of ambient particulate matter (PM) and investigate its chemical and toxicological properties, by means of oxidative potential. Different instruments such as an automatic low-volume sampler, an aethalometer and an optical particle counter, were employed for the measurement of $PM_{2.5}$ mass concentration, equivalent black carbon (eBC) concentration and absorption Ångström exponent (AAE), and particle number size distribution in 0.25–31 μm size range, respectively. 108 daily PM samples, collected on quartz fibre filters, were chemically analysed. Organic (OC) and elemental (EC) carbon content was estimated by thermo-optical transmittance technique (TOT), the concentrations of the main water-soluble ions and total elements were determined by ion chromatography and ED-XRF technique, while the oxidative potential of the water-soluble fraction was estimated through the dithiothreitol (DTT) assay. The mean value of $PM_{2.5}$ mass concentration was 9.2 ± 2.5 μg/m^3 and the average contribution of measured species on $PM_{2.5}$ mass was 3.3% EC; 19.3% OC; 27.0% secondary inorganic aerosol (sum of SO_4^{2-}, NH_4^+ and NO_3^-), and 10.2% of the other ions and elements. The OC and EC contributions to $PM_{2.5}$ mass and their mean ratio (OC/EC = 6.6 ± 3.1) suggest that the site is affected by the combined contribution of traffic emissions and biomass combustion (domestic heating and agricultural activities), with the latter prevailing over the traffic, as supported by the mean AAE value of 1.3. The mean OP normalized by sampled volume, OP_{DTTV}, was as high as 0.34 ± 0.22 nmol/min·m^3, a value comparable to those recorded for $PM_{2.5}$ in suburban areas of Italy. The correlation between OP_{DTTV} and the chemical species observed in the $PM_{2.5}$ samples showed a good agreement with the carbonaceous component OC ($r = 0.62$) and with some ions, K^+ and SO_4^{2-} ($r = 0.60$). These results identify combustion sources as the most responsible for the relatively high OP_{DTTV} activity of $PM_{2.5}$ recorded in this area.

* Corresponding author.
E-mail address: caterinamapelli@cnr.it (C. Mapelli).

https://doi.org/10.1016/j.atmosenv.2024.120656
Received 5 February 2024; Received in revised form 15 May 2024; Accepted 11 June 2024
Available online 14 June 2024

Fig. 1. Geographical location of the measurement site. The map was retrieved from Google (map data © 2023).

1. Introduction

In recent years, studies addressing particulate pollution have become a focal point for the atmospheric research community (Liu et al., 2022; Singh et al., 2022), mainly because of the increase of PM emissions in areas where abatement strategies were not effective, together with the growing awareness on the adverse environmental and health effects (Hou et al., 2023; Moreno-Ríos e al., 2021). Particulate matter is usually made up of a mixture of heterogenous components from natural and anthropogenic sources (Potter et al., 2021) that include combustion sources, industrial processes, forest and agricultural activities, construction, and fertilizer operations. These heterogeneous and dynamic mixtures of particles, have harmful effects that are strongly linked to their size and chemical composition. Together with emissions strengths, many factors can influence the local air quality, such as meteorological factors and physical-chemical transformations (Liang and Gong, 2020). Most studies on air quality analyse data collected in cities or metropolitan areas (Faustini et al., 2011; Meng et al., 2021) where the habits of the population and the origin of the main air pollutants are often different from those of non-urban areas. Accordingly, the relation between air pollution and human health may be different between urban and non-urban areas (Liu et al., 2021), and the estimation of health effects in areas characterised by low concentrations of emissions might affect the epidemiological findings. Among air pollutant emission origins, agricultural activities, domestic heating, and wildfire (forest fires) are predominant in rural areas as demonstrated by the case studies in European countries (Grange et al., 2020; Hall et al., 2021; Papadakis et al., 2015). All these sources significantly contribute to air pollution because of the emissions of carbon monoxide and dioxide, black carbon, brown carbon, sulphur dioxide, and nitrous oxides (Haszpra et al., 2022; Methymaki et al., 2023; Santiago-De La Rosa et al., 2018). An accurate monitoring of biomass burning emissions from these sources is essential in regional air quality analyses, particularly for the Mediterranean area, where future climate scenarios predict a hotter and drier climate over the next century (Zanis et al., 2014). However, there's a lack of studies regarding the estimation of the oxidative potential of PM fine fraction in the mediterranean basin. Moved by this motivation, in the context of OT4Clima (Development of Innovative Earth Observation Technologies for the Study of Climate Change and Its Impacts on the Environment), a measurement campaign was carried out between February and October 2020 in a coastal semi-rural site of Basilicata, in Southern Italy. In this study, the impact of different emission sources on the chemical properties and on the oxidative potential of the fine fraction of particulate matter ($PM_{2.5}$) was investigated in a semi-rural area. To the best of our knowledge, only a few research studies have evaluated oxidative potential of $PM_{2.5}$ in Italy, especially in rural areas, whereas most literature data focused on OP of PM_{10} in urban or highly polluted sites (Pietrogrande et al., 2019). Therefore, the results of this study represent a peculiarity as well as an important contribution for a deeper understanding of the potential health-related impact of aerosol in this environment.

2. Materials and methods

2.1. Site description and sampling strategy

The study was conducted in the Metaponto coastal plain (40°39′ N; 16°78′ E), (Fig. 1), in Southern Italy, whithin an area that represents the main agricultural land of the Basilicata region (Coluzzi et al., 2019). A mobile laboratory, equipped with different instruments, was set up in the agricultural area of ALSIA (Regional Agency for Development and Innovation in Agriculture). The site is covered by numerous and extensive green areas made up of Mediterranean scrub and cultivated fields. In particular, a Pinus halepensis forest extends almost continuously over the Ionic coastal line for about 50 km from the North-Eastern to the South-Western direction in that area. It is approximately 40 km from the most important urban centres, 6 km from the Ionic coast and about 800 m away from a state road subject to moderate traffic volumes that include both light and heavy vehicles. For this reason, the site was identified as 'semi-rural'.

Furthermore, the site is affected by contributions from medium-and long-range air masses transported from surrounding regions and from Africa (Chirizzi et al., 2017).

The measurement campaign started in February 2020, but was

stopped at the beginning of March due to the lockdown for the COVID-19 pandemic. Sampling then resumed in June together with most research activities and concluded in October 2020. It is possible that COVID-19 mitigation strategies, which were still enforced in Italy in summer 2020, somehow affected the campaign results by significantly altering human actions (Conte et al., 2020, 2023).

During the period studied, daily $PM_{2.5}$ samples (starting from midnight) were collected at low-volume (2.3 m^3/h) using an Explorer Plus (Zambelli) sampler equipped with quartz filters (Whatman Q-grade, 47 mm in diameter), pre-heated for 2 h at 700 °C before use to reduce carbon contamination.

After sampling, all $PM_{2.5}$ samples were stored in the fridge (at 4 °C) until the laboratory analysis.

$PM_{2.5}$ concentration was determined via gravimetric method with a Sartorious Cubis microbalance (±1 μg), and the uncertainties over the daily concentrations were about 10% on average.

An optical particle counter (OPC Grimm 11-A) was used to measure the particle number concentration in the size range from 0.25 to 31 μm, distributed within 31 size channels, working at controlled flow of 1.2 L/min. Measurements of equivalent black carbon (eBC) were done with a MAGEE aethalometer (AE33 model), described in detail in Pavese et al. (2020). The instrument was equipped with a $PM_{2.5}$ head, and 7 lamps which allowed to estimate the absorption Ångström exponent by means of a best-fit procedure, as described in Esposito et al. (2012).

Meteorological parameters such as rain, relative humidity (RH), temperature (T), wind speed (WS) and direction (WD) were collected by ALSIA. The weather conditions during the whole campaign were predominantly characterized by sunny days, with monthly average temperatures between 10.5 °C and 26.0 °C, relative humidity between 55% and 77%, and only June characterized by more abundant rainfall (48 mm). The dominant wind direction was from N-NW (65% of occurrence frequency) with a wind speed between 1.9 m/s and 2.7 m/s (Fig. S1).

2.2. Measurements methods

All 108 $PM_{2.5}$ samples, were chemically analysed. Each filter was sectioned into four quarters. One quarter of the filter (1 cm^2 punch) was designated to the estimation of elemental carbon (EC) and organic carbon (OC) concentrations using the thermo-optical analysis (Sunset OC/EC Analyser), operating with the EUSAAR2 protocol (Cavalli et al., 2010). Before the measurements, a multipoint calibration was carried out with an external standard sucrose solution, as described in detail by Merico et al. (2019). OC/EC values were corrected by the concentrations obtained for blank filters, which were analysed through the same method. The content of secondary organic carbon (SOC) was quantified with the EC trace method (more details in Pio et al., 2011; Turpin and Huntzicker, 1995):

$$SOC = OC - EC\left(\frac{OC}{EC}\right)_{min} \quad (1)$$

with $\left(\frac{OC}{EC}\right)_{min}$ the minimum ratio between OC and EC equal to 2.3.

Another quarter of filter was employed for High-Performance Ion Chromatography (Dionex DX600 IC system – 125 μL injection loop) to determine the concentration of water-soluble ions. Filters were extracted in two ultrasonic bath extractions of 30 min each, in 15 mL of Milli-Q water (18 MΩ). Separation of anions (Cl^-, NO_3^-, Br^-, SO_4^{2-}, $C_2O_4^{2-}$) was carried out with a Dionex IonPac AS23 analytical column (250 × 4 mm id) coupled with Dionex IonPac AS23 guard column (50 × 4 mm id) and 4.5 mM Na_2CO_3 and 1.1 mM $NaHCO_3$ as eluent in isocratic mode with a flow rate of 1.0 mL/min. Separation of cations (K^+, NH_4^+) were obtained using a Dionex IonPac CS12A analytical column (250 × 4 mm id) coupled with Dionex IonPac CG12A guard column (50 × 4 mm id) and 20 mM methane sulfonic acid (MSA) as eluent in isocratic mode with a flow rate of 1.2 mL/min. More details on the HP-IC method were provided by Cesari et al. (2018a). The detection limits (μg/L) were the followings: 33 (K^+), 7 (NH_4^+), 5 (Cl^-), 2 (NO_3^-), 2 (Br^-), 5 (SO_4^{2-}), and 2 ($C_2O_4^{2-}$). The average concentrations were corrected by those measured on blank filters.

The third quarter was used for the characterization of elements by Energy Dispersive X-ray Fluorescence spectrometry technique (ED-XRF, Spectro Xepos analyser). The filters were assembled into 32 mm sample cups supported by a double layer of mylar thin film, and a set of 10 field blanks was also analysed with the same preparation. Measurement conditions were optimised for the determination of 12 elements, i.e., Al, Ca, Cr, Cu, Fe, Mg, Mn, Na, Pb, Sr, Ti, Zn. All elements were calibrated via an external calibration based on 23 Micromatter thin film standards and a matrix calibration based on intercomparison conducted on simultaneous PM sampling on Teflon and quartz filters. The average elemental composition measured for blank samples was subtracted from the one of the sample filters and net concentrations for each element were determined in μg/m^3. The detection limit was element-dependent and for data below this threshold, values were replaced with half of the detection limit. The typical uncertainty was estimated by repeatability test, and it was, on average, less than 5% (i.e. the nominal uncertainty of the calibration standards).

Enrichment factors were estimated using the average composition of earth's upper crust as defined by Wedepohl (1995), according to equation:

$$EF_x = \frac{\left(C_x/C_{ref}\right)_{PM2.5}}{\left(C_x/C_{ref}\right)_{UC}} \quad (2)$$

where c_x represents the average concentration of element x and c_{ref} the average concentration of the reference element. The ratio of c_x and c_{ref} of the $PM_{2.5}$ samples were divided by the analogous average ratio reported by Wedepohl (1995) for the upper crust (UC).

A portion of the last quarter was tested with the dithiothreitol (DTT) assay following a protocol adapted from Cho et al. (2005) and described in detail by Chirizzi et al. (2017). Each filter was extracted in 15 mL of deionized water (DI, Milli-Q; >18 MΩ) and the extracts were filtered via polytetrafluoroethylene (PTFE) syringe filters to clean the water-soluble fraction from insoluble compounds and other residual material. A small volume (<30 μl) of stock extracted solution was incubated at 37 °C with a DTT solution and a potassium phosphate buffer for 5–90 min. At selected intervals of time, 0.2 mL of incubation mixture were collected, and the reaction was quenched with a solution of trichloroacetic acid. Finally, a solution of tris–HCl, EDTA and DTNB was added to the reaction mixture. The concentration of 5-mercapto-2-nitrobenzoic acid was then observed at 412 nm with an Omega Star spectrophotometer to indirectly estimate the concentration of DTT. The rate of DTT depletion was determined from the linear regression of absorbance versus time and was corrected according to the results obtained for the field blanks. For each sample, the assay was replicated three times, and the standard deviation was around 10%. The OP was then expressed in terms of DTT-activity normalized by sampled air volume (DTT_V). Acting as a surrogate of cellular antioxidants, DTTv could be considered as an indicator for health-related effects of PM. However, this acellular assay might be particularly sensitive to some chemical species more than others and correlations with in vitro toxicological effects were found to be site dependent (Guascito et al., 2023).

3. Results and discussions

3.1. $PM_{2.5}$ concentration and carbonaceous fraction

Daily $PM_{2.5}$ mass concentrations showed high variability (1.8–23.4 μg/m^3) with monthly values between 7.3 ± 4.0 μg/m^3 in June and October, 9.0 ± 3.7 μg/m^3 in February and July, and 10.9 ± 3.1 μg/m^3

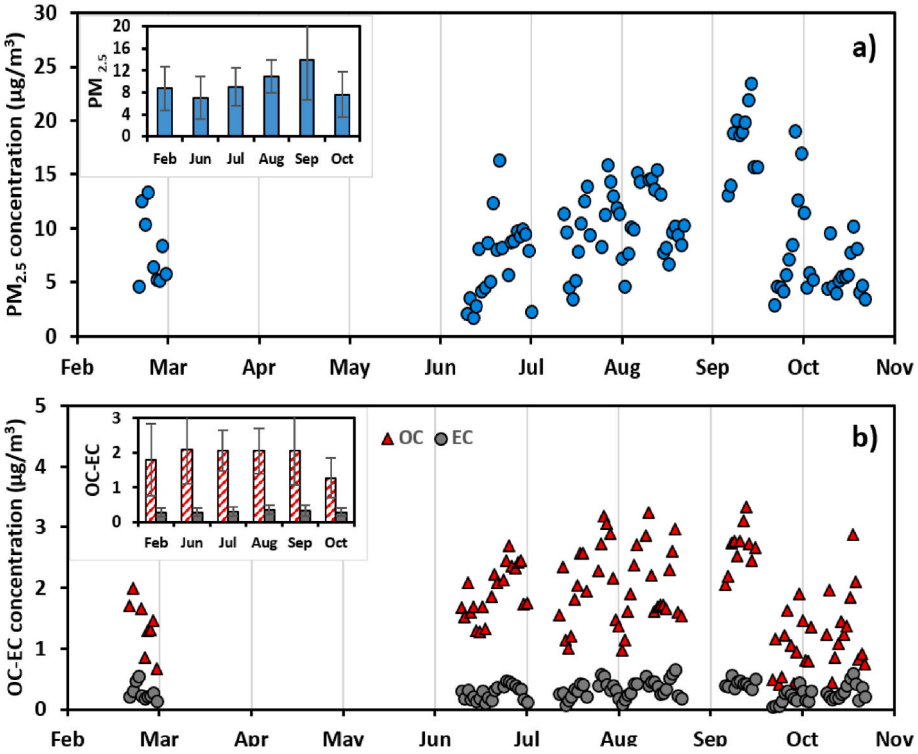

Fig. 2. Concentrations of $PM_{2.5}$ and OC/EC recorded during the campaign. (a) Daily (blue circles) and monthly (inset bar chart showing bars ± standard deviation) mass concentrations of $PM_{2.5}$. (b) Daily concentration of OC (red triangles) and EC (grey circles) and inset bar chart showing the monthly concentration of OC (red and white striped bars) and EC (grey bars).

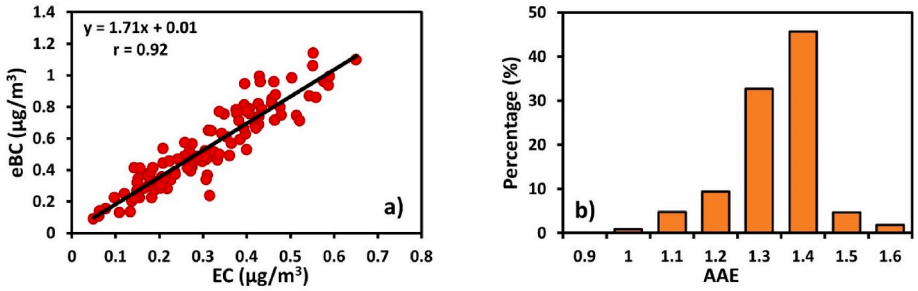

Fig. 3. Correlation of eBC with EC and AAE. (a) Scatter-plot eBC vs EC for daily data and (b) AAE histogram for daily data.

and 13.9 ± 7.1 μg/m^3 in August and September, respectively (Fig. 2a). The mean value over the entire period was 9.5 ± 4.8 μg/m^3, very close to the 9.19 μg/m^3 mean value obtained by Malaguti et al., 2015 for a two-months measurements campaign in a coastal site situated about 26 km South-West from the study area. The low PM concentrations observed in June, as shown in Fig. 2a, could be related to the higher rainfall recorded during this month, while the higher concentrations of September could be due to the combustion of biomass in agricultural practices. These activities release primary particulate matter, among which carbonaceous species that favour the formation of secondary organic aerosol as observed in Fig. 5b. A possible contribution of desert dust was excluded both by studying the back trajectories of the air masses and the local wind conditions, which confirmed the wind blew mainly from the north-northwest sector with average speeds of 2.7 m/s (Fig. S1) in those days.

The average OC and EC mass concentrations were 1.9 ± 0.8 μg/m^3 and 0.3 ± 0.1 μg/m^3, respectively, with average monthly concentrations almost constant during the entire period, except in October when the OC value was lower (Fig. 2).

The results of the EC/eBC comparison reported in Fig. 3a show how, despite the different measurements techniques, there was a good correlation (r = 0.92) between those parameters, supporting the usage of AAE in detecting BC and BrC, that is the absorbing fraction of OC (Lack and Langridge, 2013).

Fig. 3b shows the histogram of AAE values: 78.5% of AAEs were between 1.3 and 1.4, suggesting a constant contribution of BrC possibly produced both by domestic heating and biomass burning from agricultural activities (Pavese et al., 2022). This contribution was particularly relevant in the months of February and September, when AAE vs. OC showed, respectively, a correlation r = 0.69 and r = 0.81 (Figs. S2a and S2b).

Daily SOC concentrations (Fig. S3) exhibited a wide variability, between 0.5 and 5.0 μg m^{-3}, with monthly values ~1.3 μg/m^3 (except October 0.6 μg/m^3) and accounting for a large percentage (~60%) of the OC mass. This highlights the different primary and secondary sources of organic carbon, in good agreement with the results of the correlation analysis of OC vs EC. The large proportion of SOC can be explained with an increase of organic precursor emissions and/or with the intensification of photochemical oxidation due to the higher solar radiation in the warm months.

Table 1
Mean ± standard deviation, minimum and maximum values of concentrations, expressed in μg/m3 (*nmol/min·m^3) of the different chemical species measured.

	Mean	St. Dev	Min	Max
$PM_{2.5}$	9.5	4.8	1.8	23.4
OC	1.84	0.75	0.41	4.15
EC	0.31	0.14	0.05	0.65
SO_4^{2-}	1.92	1.51	0.32	7.31
NO_3^-	0.42	0.21	0.11	1.10
NH_4^+	0.25	0.23	0.01	0.83
Cl^-	0.16	0.24	0.01	2.06
K^+	0.12	0.09	0.01	0.67
Br −	0.002	0.001	0.001	0.007
OXA	0.19	0.09	0.004	0.40
Na	0.085	0.083	0.008	0.433
Mg	0.023	0.018	0.003	0.083
Ca	0.213	0.017	0.012	0.831
Al	0.073	0.061	0.003	0.246
Ti	0.012	0.009	0.0004	0.038
Cr	0.0004	0.0004	0.0001	0.003
Mn	0.003	0.002	0.0001	0.011
Fe	0.083	0.059	0.007	0.247
Cu	0.003	0.002	0.001	0.011
Zn	0.012	0.018	0.002	0.185
Sr	0.001	0.001	0.0002	0.004
Pb	0.003	0.002	0.0002	0.014
SOC	1.16	0.64	0.05	5.00
DTTv*	0.34	0.22	0.02	1.05

The overall particle number concentration ranged between 67 × 10^3 L^{-1} in October and 188 × 10^3 L^{-1} in September, with a mean value of 130 × 10^3 L^{-1}. The number size distributions profiles were similar from month to month (Fig. S4) and were represented by a bimodal distribution with a first mode within the 0.25–0.8 μm range, and a maximum at around D ~ 0.3 μm, in proximity of the lower detection limit. A second mode was observed around 1.8 μm, in February, September and October, and 2.2 μm in the other months, but was more pronounced in August whit dimensions approximately 30% higher than those in June and July. This shift towards larger particles can be ascribed to the insolation and dryness that characterize the Mediterranean summers (Pikridas et al., 2018) and which would facilitate the resuspension of coarse particles especially in rural areas (Orza et al., 2011).

3.2. Chemical composition and correlation

The concentration of the measured chemical species represented about 60 % of $PM_{2.5}$ mass. The most abundant species and the corresponding average distribution were 3.3% EC, 19.3% OC, 27.0% sum of SO_4^{2-}, NH_4^+ and NO_3^- (ions associated with secondary inorganic aerosol, SIA) and 10.2% sum of the other chemical species.

The mean values (± standard deviation) and the minimum and maximum range of $PM_{2.5}$ concentration, carbon content, OP_V^{DTT}, ions and elemental concentration were listed in Table 1. Moreover, the relationship between the different species was expressed by Pearson's coefficients (r) reported in Table S1.

Among the ions, SO_4^{2-} had the highest mean concentration (1.92 ± 1.51 μg m^{-3}), followed by NO_3^- (0.42 ± 0.21 μg m^{-3}), NH_4^+ (0.25 ± 0.23 μg m^{-3}), Cl^- (0.16 ± 0.24 μg m^{-3}) and K^+ (0.12 ± 0.01 μg m^{-3}).

Fig. 4 shows the monthly percentage composition of $PM_{2.5}$ with respect to the observed ionic species. Monthly variability indicates that the contribution of chloride and nitrate decreases during the warmer months because of thermal instability, while that of ammonium, sulphate and oxalate was larger during the warmer months compared to the colder one (February and October) because their formation is accelerated by strong solar radiation and high relative humidity. Similar behaviour was also observed for K^+.

The relationship between the different chemical species provided additional information on the sources that characterized the collected PM. In fact, the strong correlation ($r = 0.85$, $p < 0.05$) between $SO_4^{2-}$and NH_4^+ and the high ratio SO_4^{2-}/NH_4^+ suggests that secondary sulphate was present as both ammonium sulphate and bisulphate (Cesari et al., 2018a), and ammonium ions were not sufficient to neutralise sulphate and nitrate.

The OC vs EC mass concentrations were found to be well correlated (Pearson's $r = 0.80$, $p < 0.05$ excluding 22 June, otherwise $r = 0.69$) suggesting that OC and EC were emitted by shared primary sources (Contini et al., 2018). Also, the OC/EC mean value was 6.6 ± 3.1, ranging from 4.7 in October and exhibiting higher monthly mean values in June (8.5) and July (7.6). As known, this ratio strongly depends on the distance from the emission sources and combination of road traffic and biomass combustion and can vary from values as low as 1in polluted environments, up to 15 in remote areas (Sandrini et al., 2014). It is estimated a ratio between 1.4 and 5 for gasoline emissions and between 0.3 and 1 for diesel emissions (Amato et al., 2016; Cesari et al., 2018b; Salameh et al., 2015), while ratios from 5 to 12 are expected for biomass burning (Szidat et al., 2006). In this case, the ratios could be attributed to the combined effects of vehicle exhaust emissions and biomass combustion. The sampling site is located about 1 km from an arterial road, which explain the contribution of motor vehicle exhaust

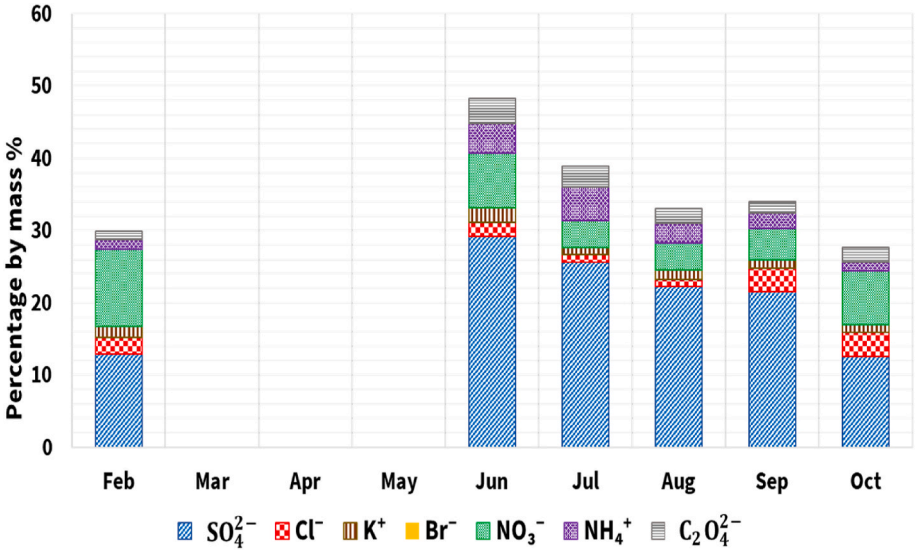

Fig. 4. HP-IC analysis results. Monthly average concentration expressed in percentage by mass for the 12 elements measured by HP-IC.

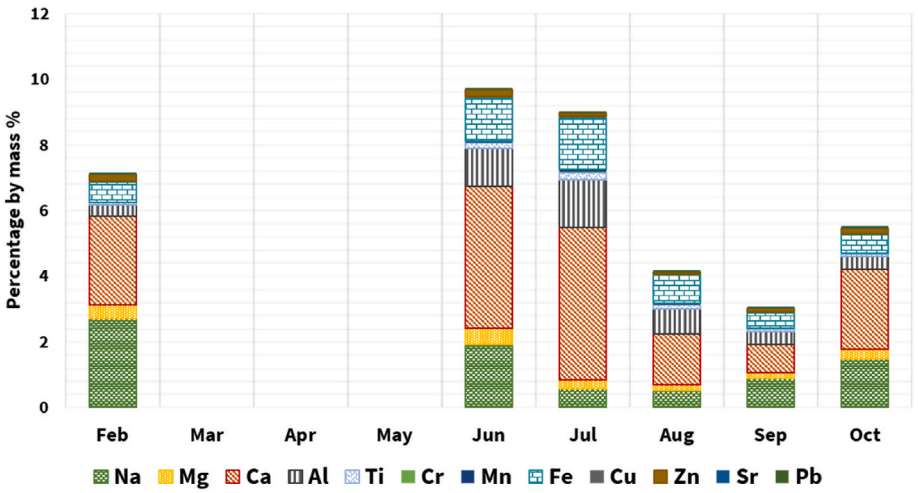

Fig. 5. ED-XRF analysis results. Monthly average concentration expressed in percentage by mass for the 12 elements measured by ED-XRF.

emissions. At the same time the presence of biomass burning emissions was supported by the good correlation ($r = 0.76$, $p < 0.05$) found between OC concentrations and K^+, which has been extensively employed as a tracer of biomass burning (Almeida et al., 2006; Li et al., 2003; Yu et al., 2018). Although no wildfires phenomena were identified, it is likely that brushwood and stubble were burned as usual agricultural practices in these areas, also during the spring and summer months.

ED-XRF analysis showed that calcium was the most abundant element (0.213 ± 0.017 μg m^{-3}) followed by Na (0.085 ± 0.083 μg m^{-3}), Fe (0.083 ± 0.059 μg m^{-3}), Al (0.073 ± 0.061 μg m^{-3}) and Mg (0.023 ± 0.018 μg m^{-3}) as expected for particulate matter deriving from soil rich in limestone and from the proximity to the coast. Concentrations of Al and other typical crustal elements such as Fe, Ti and Mn were strongly correlated ($r > 0.80$, $p < 0.05$), suggesting common origin from soil erosion and resuspension that could also be related to agricultural activities typical of the area of study. Except for Na^+, the monthly percentage by mass shown in Fig. 5 revealed a common trend for these elements, with an increase of concentration in the summer months, typically due to the dryness of the soil. Good correlation was also observed between Mg and Na ($r = 0.73$, $p < 0.001$) and between Cl- and Mg ($r = 0.47$, $p < 0.001$) and Na ($r = 0.55$, $p < 0.001$), probably deriving from sea-spray sources. Assuming that all Na and Cl were coming up from marine origin, the sea-spray concentration could be estimated using the formula sea-spray = 1.4468[Na] + [Cl^-] (Maenhaut et al., 2008), to obtain a value of 0.27 μg/m^3, that is 2.9% of the $PM_{2.5}$ concentration, value in agreement with the means observed for other coastal sites of the Mediterranean area (Cesari et al., 2012; Pey et al., 2009). A deeper look to the day-by-day sea-spray concentration showed that marine contribution remained as low as 0.2 μg/m^3 for most of the time except for a couple of days in autumn, reaching a maximum around the 3rd of October.

Assuming that Na was originated solely from marine spray, the sea-spray contributions were subtracted from Na and Mg concentrations, and the enrichment factors were estimated for Ca non-sea salt (n_{ss}), for Mg (n_{ss}), and for all the other elements measured, using Fe as reference (Fig. S5). EFs were analysed using a threshold of 4 defined by Cesari et al. (2012). Cu, Zn and Pb were the only elements showing a significant enrichment which indicates a likely anthropogenic source, while the EF estimated for Cr suggests both crustal and anthropogenic origin.

3.3. Oxidative potential

The OP responses normalized by the volume of sampled air, DTT_V, were reported in Table 1 while the time series was represented in Fig. 6.

The average OP was 0.34 ± 0.22 nmol/min·m^3, ranging from 0.02 nmol/min·m^3 to 1.05 nmol/min·m^3 daily values (Fig. 6) and from 0.22 nmol/min·m^3 (in February) to 0.57 nmol/min·m^3 (in September) monthly means (red bars in Fig. 6). The wide variability of the DTT_V can be linked to the daily change in the concentration and composition of $PM_{2.5}$ that characterizes this site, affected by the long-range transport of pollutants from neighbouring regions (Perrone et al., 2019).

This is supported by the fact that at high DTT_V corresponded large $PM_{2.5}$ concentrations, as evidenced by the good correlation ($r = 0.72$ p < 0.005).

In fact, it is interesting to observe that, although the area of study is representative of a rural environment, far from large sources of industrial or urban emissions, the values found were comparable, or even larger than those observed in other studies concerning the $PM_{2.5}$ fraction in suburban areas in Italy (Cesari et al., 2019; Chirizzi et al., 2017; Giannossa et al., 2022; Perrone et al., 2019; Pietrogrande et al., 2023) and lower than those observed in typical European rural areas (in 't Veld et al., 2023; Vörösmarty et al., 2023). The two sites of southern Italy where the oxidative potential of the fine fraction of PM was previously investigated, the sites of Lecce (Giannossa et al., 2022) and Sarno (Cesari et al., 2019), represent respectively an urban and an industrial area. Although both sites recorded a much larger concentration of $PM_{2.5}$ compared to this work, DTTv values were smaller than the 0.34 nmol/min·m^3 measured for Metaponto (DTTv (Lecce) = 0.29 nmol/min·m^3 and DTTv (Sarno) = 0.29 nmol/min·m^3).

In this regard, to identify the pollution sources linked to this surprisingly intense OP activity, DTT_V values were investigated and related to the chemical composition of the PM through correlation analysis with the chemical species analysed. As can be seen from the Pearson coefficients (r) reported in Table 2, the DTT_V showed significant correlation with only few species. In particular, good correlation was found with OC ($r = 0.62$), EC ($r = 0.44$), and K^+ ($r = 0.60$) that are commonly associated with emissions from combustion sources (Matawle et al., 2015). Noteworthy were also the correlations with NH_4^+ ($r = 0.50$), SO_4^{2-} ($r = 0.61$), oxalate ($r = 0.52$), and SOC ($r = 0.63$) indicating that photochemical aging processes could also affect the toxicity of PM (Kodros et al., 2020) and secondary aerosol could be responsible for the OP activity (Cesari et al., 2019; in 't Veld et al., 2023).

These results are in agreement with recent literature studies on $PM_{2.5}$, reporting carbonaceous aerosols as the main OP contributors (Fang et al., 2016; Lyu et al., 2018; Moreno et al., 2017; Perrone et al., 2019; Shirmohammadi et al., 2017; Styszko et al., 2017; Zhang et al., 2017). The seasonality of DTTv, characterised by higher values in the cold months, was well correlated with an increase of emissions from combustion sources and suggests an association of OP with winter sources. In this work, the lack of winter data did not allow to support

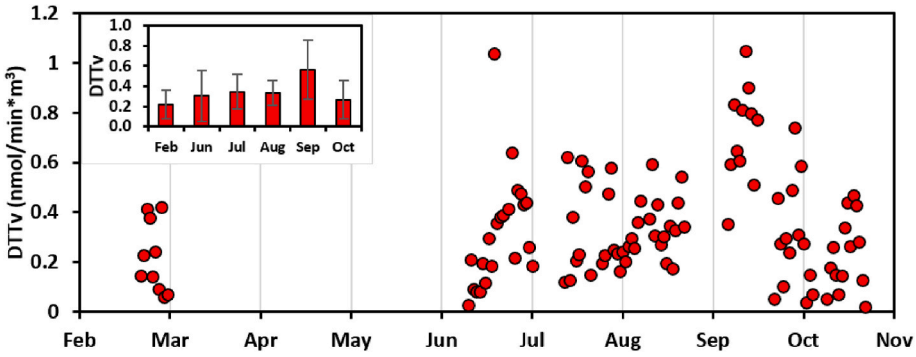

Fig. 6. OP values obtained via DTT assay expressed in DTTv. Daily (red circles) and monthly (red bars) volume normalized DTTv activity of the collected $PM_{2.5}$ samples.

this, but the significant correlation observed with carbonaceous fraction of PM suggests the influence of common sources such as the combustion of biomass and traffic emissions (Fig. 6).

4. Conclusions

In this study, the physico-chemical composition of atmospheric aerosol collected in a coastal semi-rural site of southern Italy was analysed, and its OP was estimated via the acellular DTT assay. The mean mass concentration of $PM_{2.5}$ was 9.2 ± 2.5 μg/m^3 with an average contribution of measured species of 3.3% for EC, 19.3% for OC, 27.0% for secondary inorganic aerosol, and 10.2% for the other water-soluble ions and elements. The $PM_{2.5}$ mass and composition can be traced back to the specific sources characterizing the site. The notable proportion of carbonaceous species, as well as the high mean AAE value of 1.3, indicate that the site is affected by the combined contribution of traffic emissions and biomass combustion, including both the domestic heating and the agricultural activities. Despite low $PM_{2.5}$ mass concentrations, the mean value of OP normalized by volume was 0.34 ± 0.22 nmol/min·m^3, comparable to values observed from some suburban areas. The high correlation of OP with $PM_{2.5}$ mass concentration ($r = 0.72$) reflects the contribution of specific $PM_{2.5}$ components, as highlighted by the correlations with organic carbon ($r = 0.62$), and K^+ and SO_4^{2-} ($r = 0.60$) ions, suggesting that combustion activities are one of the main sources responsible for the OP activity of $PM_{2.5}$ at this specific site. This study highlights that fine particulate matter can have a noticeable impact on environment and health, even in areas not strongly influenced by anthropogenic sources, and that PM mass concentrations alone is not a valid indicator of air quality in terms of potential effects on health. However, without a clear identification of an involved sources, their actual impact on human health cannot be accurately determined.

Therefore, in addition to this study more extensive monitoring campaigns will be needed to investigate the factors responsible for the composition of atmospheric aerosols and their seasonal variability in this area.

In addition, the information on chemical compositions discussed in this work could be used for source apportionment studies which would provide a deeper understanding of the different contributions to the generation of PM in this site, which would be possibly representative of similar areas.

CRediT authorship contribution statement

A. Dinoi: Writing – review & editing, Writing – original draft, Supervision, Investigation, Conceptualization. **G. Pavese:** Writing – original draft, Data curation. **M. Calvello:** Writing – original draft, Data curation. **D. Chirizzi:** Writing – original draft, Formal analysis, Data curation. **A. Pennetta:** Writing – original draft, Formal analysis, Data curation. **G.E. De Benedetto:** Writing – original draft, Data curation. **F. Esposito:** Writing – original draft, Data curation. **C. Mapelli:** Writing – review & editing, Investigation, Data curation, Writing – review & editing, Writing – original draft, Formal analysis, Data curation. **D. Contini:** Writing – review & editing, Supervision, Funding acquisition, Data curation, Conceptualization.

Declaration of competing interest

The authors declare the following financial interests/personal relationships which may be considered as potential competing interests:

Daniele Contini reports financial support was provided by Ministry of Education and Merit. If there are other authors, they declare that they have no known competing financial interests or personal relationships that could have appeared to influence the work reported in this paper.

Data availability

Data will be made available on request.

Acknowledgements

The work was supported in the framework of project OT4CLIMA (Innovative Earth Observation technologies to study Climate Change and its impact on the environment- D.D. MIUR 2261 del 6.9.2018, PON R&I 2014–2020 e FSC).

The authors would like to thank ALSIA for hosting our instruments and for providing meteorological data. In particular we want to thank Dr. Emanuele Scalcione, Dr. Pietro Zienna and Mr. Cosimo De Monte who made our measurement campaign possible.

Appendix A. Supplementary data

Supplementary data to this article can be found online at https://doi.org/10.1016/j.atmosenv.2024.120656.

References

Almeida, S.M., Pio, C.A., Freitas, M.C., Reis, M.A., Trancoso, M.A., 2006. Approaching PM2.5 and PM2.5–10 source apportionment by mass balance analysis, principal component analysis and particle size distribution. Sci. Total Environ. 368, 663–674. https://doi.org/10.1016/j.scitotenv.2006.03.031.

Amato, F., Alastuey, A., Karanasiou, A., Lucarelli, F., Nava, S., Calzolai, G., Severi, M., Becagli, S., Gianelle, V.L., Colombi, C., Alves, C., Custódio, D., Nunes, T., Cerqueira, M., Pio, C., Eleftheriadis, K., Diapouli, E., Reche, C., Minguillón, M.C., Manousakas, M.I., Maggos, T., Vratolis, S., Harrison, R.M., Querol, X., 2016. AIRUSE-LIFE+: a harmonized PM speciation and source apportionment in five southern European cities. Atmos. Chem. Phys. 16, 3289–3309. https://doi.org/10.5194/acp-16-3289-2016.

Cavalli, F., Viana, M., Yttri, K.E., Genberg, J., Putaud, J.P., 2010. Toward a standardised thermal-optical protocol for measuring atmospheric organic and elemental carbon: the EUSAAR protocol. Atmos. Meas. Tech. 3, 79–89. https://doi.org/10.5194/amt-3-79-2010.

Cesari, D., Contini, D., Genga, A., Siciliano, M., Elefante, C., Baglivi, F., Daniele, L., 2012. Analysis of raw soils and their re-suspended PM10 fractions: characterisation of source profiles and enrichment factors. Appl. Geochem. 27, 1238–1246. https://doi.org/10.1016/j.apgeochem.2012.02.029.

Cesari, D., Merico, E., Grasso, F.M., Decesari, S., Belosi, F., Manarini, F., De Nuntiis, P., Rinaldi, M., Volpi, F., Gambaro, A., Morabito, E., Contini, D., 2019. Source apportionment of PM2.5 and of its oxidative potential in an industrial suburban site in south Italy. Atmosphere 10, 758. https://doi.org/10.3390/atmos10120758.

Cesari, D., De Benedetto, G.E., Bonasoni, P., Busetto, M., Dinoi, A., Merico, E., Chirizzi, D., Cristofanelli, P., Donateo, A., Grasso, F.M., Marinoni, A., Pennetta, A., Contini, D., 2018a. Seasonal variability of PM2.5 and PM10 composition and sources in an urban background site in Southern Italy. Sci. Total Environ. 612, 202–213. https://doi.org/10.1016/j.scitotenv.2017.08.230.

Cesari, D., Merico, E., Dinoi, A., Marinoni, A., Bonasoni, P., Contini, D., 2018b. Seasonal variability of carbonaceous aerosols in an urban background area in Southern Italy. Atmos. Res. 200, 97–108.

Chirizzi, D., Cesari, D., Guascito, M.R., Dinoi, A., Giotta, L., Donateo, A., Contini, D., 2017. Influence of Saharan dust outbreaks and carbon content on oxidative potential of water-soluble fractions of PM2.5 and PM10. Atmos. Environ. 163, 1–8. https://doi.org/10.1016/j.atmosenv.2017.05.021.

Cho, A.K., Sioutas, C., Miguel, A.H., Kumagai, Y., Schmitz, D.A., Singh, M., Eiguren-Fernandez, A., Froines, J.R., 2005. Redox activity of airborne particulate matter at different sites in the Los Angeles Basin. Environ. Res. 99, 40–47. https://doi.org/10.1016/j.envres.2005.01.003.

Coluzzi, R., D'Emilio, M., Imbrenda, V., Giorgio, G.A., Lanfredi, M., Macchiato, M., Ragosta, M., Simoniello, T., Telesca, V., 2019. Investigating climate variability and long-term vegetation activity across heterogeneous Basilicata agroecosystems. Geomatics, Nat. Hazards Risk 10, 168–180. https://doi.org/10.1080/19475705.2018.1513872.

Conte, M., Dinoi, A., Grasso, F.M., Merico, E., Guascito, M.R., Contini, D., 2023. Concentration and size distribution of atmospheric particles in southern Italy during COVID-19 lockdown period. Atmos. Environ. 295, 119559 https://doi.org/10.1016/j.atmosenv.2022.119559.

Conte, M., Merico, E., Cesari, D., Dinoi, A., Grasso, F.M., Donateo, A., Guascito, M.R., Contini, D., 2020. Long-term characterisation of African dust advection in south-eastern Italy: influence on fine and coarse particle concentrations, size distributions, and carbon content. Atmos. Res. 233, 104690 https://doi.org/10.1016/j.atmosres.2019.104690.

Contini, D., Vecchi, R., Viana, M., 2018. Carbonaceous aerosols in the atmosphere. Atmosphere 9, 181. https://doi.org/10.3390/atmos9050181.

Esposito, F., Calvello, M.R., Gueguen, E., Pavese, G., 2012. A new algorithm for brown and black carbon identification and organic carbon detection in fine atmospheric aerosols by a multi-wavelength Aethalometer. Atmos. Meas. Tech. Discuss. 1003–1027. https://doi.org/10.5194/amtd-5-1003-2012, 2012.

Fang, T., Verma, V., Bates, J.T., Abrams, J., Klein, M., Strickland, M.J., Sarnat, S.E., Chang, H.H., Mulholland, J.A., Tolbert, P.E., Russell, A.G., Weber, R.J., 2016. Oxidative potential of ambient water-soluble PM2.5 in the southeastern United States: contrasts in sources and health associations between ascorbic acid (AA) and dithiothreitol (DTT) assays. Atmos. Chem. Phys. 16, 3865–3879. https://doi.org/10.5194/acp-16-3865-2016.

Faustini, A., Stafoggia, M., Berti, G., Bisanti, L., Chiusolo, M., Cernigliaro, A., Mallone, S., Primerano, R., Scarnato, C., Simonato, L., Vigotti, M.A., Forastiere, F., 2011. The relationship between ambient particulate matter and respiratory mortality: a multi-city study in Italy. Eur. Respir. J. 38, 538–547. https://doi.org/10.1183/09031936.00093710.

Giannossa, L.C., Cesari, D., Merico, E., Dinoi, A., Mangone, A., Guascito, M.R., Contini, D., 2022. Inter-annual variability of source contributions to PM10, PM2.5, and oxidative potential in an urban background site in the central mediterranean. J. Environ. Manag. 319, 115752 https://doi.org/10.1016/j.jenvman.2022.115752.

Grange, S.K., Lötscher, H., Fischer, A., Emmenegger, L., Hueglin, C., 2020. Evaluation of equivalent black carbon source apportionment using observations from Switzerland between 2008 and 2018. Atmos. Meas. Tech. 13, 1867–1885. https://doi.org/10.5194/amt-13-1867-2020.

Guascito, M.R., Lionetto, M.G., Mazzotta, F., Conte, M., Giordano, M.E., Caricato, R., De Bartolomeo, A.R., Dinoi, A., Cesari, D., Merico, E., Mazzotta, L., Contini, D., 2023. Characterisation of the correlations between oxidative potential and in vitro biological effects of PM(10) at three sites in the central Mediterranean. J. Hazard Mater. 448, 130872 https://doi.org/10.1016/j.jhazmat.2023.130872.

Hall, J.V., Zibtsev, S.V., Giglio, L., Skakun, S., Myroniuk, V., Zhuravel, O., Goldammer, J. G., Kussul, N., 2021. Environmental and political implications of underestimated cropland burning in Ukraine. Environ. Res. Lett. 16, 064019 https://doi.org/10.1088/1748-9326/abfc04.

Haszpra, L., Barcza, Z., Ferenczi, Z., Hollós, R., Kern, A., Kljun, N., 2022. Real-world wintertime CO, N2O, and CO2 emissions of a central European village. Atmos. Meas. Tech. 15, 5019–5031. https://doi.org/10.5194/amt-15-5019-2022.

Hou, S., Zheng, N., Tang, L., Ji, X., Li, Y., Hua, X., 2023. Pollution characteristics, sources, and health risk assessment of human exposure to Cu, Zn, Cd and Pb pollution in urban street dust across China between 2009 and 2018. Environ. Int. 128, 430–437. https://doi.org/10.1016/j.envint.2019.04.046.

in 't Veld, M., Pandolfi, M., Amato, F., Pérez, N., Reche, C., Dominutti, P., Jaffrezo, J., Alastuey, A., Querol, X., Uzu, G., 2023. Discovering oxidative potential (OP) drivers of atmospheric PM10, PM2.5, and PM1 simultaneously in North-Eastern Spain. Sci. Total Environ. 857, 159386 https://doi.org/10.1016/j.scitotenv.2022.159386.

Kodros, J.K., Papanastasiou, D.K., Paglione, M., Masiol, M., Squizzato, S., Florou, K., Skyllakou, K., Kaltsonoudis, C., Nenes, A., Pandis, S.N., 2020. Rapid dark aging of biomass burning as an overlooked source of oxidized organic aerosol. Proc. Natl. Acad. Sci. USA 117, 33028–33033. https://doi.org/10.1073/pnas.2010365117.

Lack, D.A., Langridge, J.M., 2013. On the attribution of black and brown carbon light absorption using the Ångström exponent. Atmos. Chem. Phys. 13, 10535–10543. https://doi.org/10.5194/acp-13-10535-2013.

Li, J., Pósfai, M., Hobbs, P.V., Buseck, P.R., 2003. Individual aerosol particles from biomass burning in southern Africa: 2, Compositions and aging of inorganic particles. J. Geophys. Res. Atmos. 108 https://doi.org/10.1029/2002JD002310.

Liang, L., Gong, P., 2020. Urban and air pollution: a multi-city study of long-term effects of urban landscape patterns on air quality trends, Scientif. Rep 10, 18618. https://doi.org/10.1038/s41598-020-74524-9.

Liu, L., Fang, J., Li, M., Hossin, M.A., Shao, Y., 2022. The effect of air pollution on consumer decision making: a review. Clean. Eng. Technol. 9, 100514 https://doi.org/10.1016/j.clet.2022.100514.

Liu, T., Meng, H., Yu, M., Xiao, Y., Huang, B., Lin, L., Zhang, H., Hu, R., Hou, Z., Xu, Y., Yuan, L., Qin, M., Zhao, Q., Xu, X., Gong, W., Hu, J., Xiao, J., Chen, S., Zeng, W., Li, X., He, G., Rong, Z., Huang, C., Du, Y., Ma, W., 2021. Urban-rural disparity of the short-term association of PM2.5 with mortality and its attributable burden. Innovation 2, 100171. https://doi.org/10.1016/j.xinn.2021.100171.

Lyu, Y., Guo, H., Cheng, T., Li, X., 2018. Particle size distributions of oxidative potential of lung-deposited particles: assessing contributions from quinones and water-soluble metals. Environ. Sci. Technol. 52, 6592–6600. https://doi.org/10.1021/acs.est.7b06686.

Maenhaut, W., Raes, N., Chi, X., Cafmeyer, J., Wang, W., 2008. Chemical composition and mass closure for PM2.5 and PM10 aerosols at K-puszta, Hungary, in summer 2006. X Ray Spectrom. 37, 193–197. https://doi.org/10.1002/xrs.1062.

Malaguti, A., Mircea, M., La Torretta, T.M.G., Telloli, C., Petralia, E., Stracquadanio, M., Berico, M., 2015. Comparison of Online and Offline Methods for Measuring Fine Secondary Inorganic Ions and Carbonaceous Aerosols in the Central Mediterranean Area. Aerosol Air Qual. Res. 15, 2641–2653. https://doi.org/10.4209/aaqr.2015.04.02402015.

Matawle, J.L., Pervez, S., Dewangan, S., Shrivastava, A., Tiwari, S., Pant, P., Deb, M.K., Pervez, Y., 2015. Characterization of PM2.5 source profiles for traffic and dust sources in raipur, India. Aerosol Air Qual. Res. 15, 2537–2548. https://doi.org/10.4209/aaqr.2015.04.0222.

Meng, Y., Li, Y., Liu, H., Huang, Y., 2021. Study on evaluation of urban and rural high-quality living space based on accessibility analysis——taking shahe city, hebei province as an example. IOP Conf 769, 022075. https://doi.org/10.1088/1755-1315/769/2/022075.

Merico, E., Cesari, D., Dinoi, A., Gambaro, A., Barbaro, E., Guascito, M.R., Giannossa, L. C., Mangone, A., Contini, D., 2019. Inter-comparison of carbon content in PM10 and PM2.5 measured with two thermo-optical protocols on samples collected in a Mediterranean site. Environ. Sci. Pollut. Res. 26, 29334–29350. https://doi.org/10.1007/s11356-019-06117-7.

Methymaki, G., Bossioli, E., Boucouvala, D., Nenes, A., Tombrou, M., 2023. Brown carbon absorption in the Mediterranean basin from local and long-range transported biomass burning air masses. Atmos. Environ. 306, 119822 https://doi.org/10.1016/j.atmosenv.2023.119822.

Moreno-Ríos, A.L., Tejeda-Benítez, L.P., Bustillo-Lecompte, C.F., 2022. Sources, characteristics, toxicity, and control of ultrafine particles: an overview. Geosci. Front. 13, 101147 https://doi.org/10.1016/j.gsf.2021.101147.

Moreno, T., Kelly, F.J., Dunster, C., Oliete, A., Martins, V., Reche, C., Minguillón, M.C., Amato, F., Capdevila, M., de Miguel, E., Querol, X., 2017. Oxidative potential of subway PM2.5, Atmos. Environ. Times 148, 230–238. https://doi.org/10.1016/j.atmosenv.2016.10.045.

Orza, J.A.G., Cabello, M., Lidón, V., Martínez, J., 2011. Contribution of resuspension to particulate matter inmission levels in SE Spain. J. Arid Environ. 75, 545–554. https://doi.org/10.1016/j.jaridenv.2011.01.006.

Papadakis, G.Z., Megaritis, A.G., Pandis, S.N., 2015. Effects of olive tree branches burning emissions on PM2.5 concentrations. Atmos. Environ. 112, 148–158. https://doi.org/10.1016/j.atmosenv.2015.04.014.

Pavese, G., Calvello, M., Castagna, J., Esposito, F., 2020. Black carbon and its impact on air quality in two semi-rural sites in Southern Italy near an oil pre-treatment plant. Atmos. Environ. 233, 117532 https://doi.org/10.1016/j.atmosenv.2020.117532.

Pavese, G., Agresti, F., Calvello, M., Esposito, F., Lettino, A., 2022. Outdoor and indoor measurements of number particles size distributions and equivalent black carbon (EBC) at a mechanical manufacturing plant. Atmos. Pollut. Res. 13, 101488 https://doi.org/10.1016/j.apr.2022.101488.

Perrone, M.R., Bertoli, I., Romano, S., Russo, M., Rispoli, G., Pietrogrande, M.C., 2019. PM2.5 and PM10 oxidative potential at a Central Mediterranean Site: contrasts between dithiothreitol- and ascorbic acid-measured values in relation with particle size and chemical composition. Atmos. Environ. 210, 143–155. https://doi.org/10.1016/j.atmosenv.2019.04.047.

Pey, J., Querol, X., Alastuey, A., 2009. Variations of levels and composition of PM10 and PM2.5 at an insular site in the Western Mediterranean, Atmos. Res. 94, 285–299. https://doi.org/10.1016/j.atmosres.2009.06.006.

Pietrogrande, M.C., Russo, M., Zagatti, E., 2019. Review of PM oxidative potential measured with acellular assays in urban and rural sites across Italy. Atmosphere 10, 626. https://doi.org/10.3390/atmos10100626.

Pietrogrande, M.C., Colombi, C., Cuccia, E., Dal Santo, U., Romanato, L., 2023. Seasonal and spatial variations of the oxidative properties of ambient PM(2.5) in the Po valley, Italy, before and during COVID-19 lockdown restrictions. Int. J. Environ. Res. Publ. Health 20. https://doi.org/10.3390/ijerph20031797.

Pikridas, M., Vrekoussis, M., Sciare, J., Kleanthous, S., Vasiliadou, E., Kizas, C., Savvides, C., Mihalopoulos, N., 2018. Spatial and temporal (short and long-term) variability of submicron, fine and sub-10 μm particulate matter (PM1, PM2.5, PM10)

in Cyprus. Atmos. Environ. 191, 79–93. https://doi.org/10.1016/j.atmosenv.2018.07.048.

Pio, C., Cerqueira, M., Harrison, R.M., Nunes, T., Mirante, F., Alves, C., Oliveira, C., Sanchez de la Campa, A., Artíñano, B., Matos, M., 2011. OC/EC ratio observations in Europe: Re-thinking the approach for apportionment between primary and secondary organic carbon. Atmos. Environ. 45, 6121–6132. https://doi.org/10.1016/j.atmosenv.2011.08.045.

Potter, N.A., Meltzer, G.Y., Avenbuan, O.N., Raja, A., Zelikoff, J.T., 2021. Particulate matter and associated metals: a link with neurotoxicity and mental health. Atmosphere 12, 425. https://doi.org/10.3390/atmos12040425.

Salameh, D., Detournay, A., Pey, J., Pérez, N., Liguori, F., Saraga, D., Bove, M.C., Brotto, P., Cassola, F., Massabò, D., Latella, A., Pillon, S., Formenton, G., Patti, S., Armengaud, A., Piga, D., Jaffrezo, J.L., Bartzis, J., Tolis, E., Prati, P., Querol, X., Wortham, H., Marchand, N., 2015. PM2.5 chemical composition in five European Mediterranean cities: a 1-year study. Atmos. Res. 155, 102–117. https://doi.org/10.1016/j.atmosres.2014.12.001.

Sandrini, S., Fuzzi, S., Piazzalunga, A., Prati, P., Bonasoni, P., Cavalli, F., Bove, M.C., Calvello, M., Cappelletti, D., Colombi, C., Contini, D., de Gennaro, G., Di Gilio, A., Fermo, P., Ferrero, L., Gianelle, V., Giugliano, M., Ielpo, P., Lonati, G., Marinoni, A., Massabò, D., Molteni, U., Moroni, B., Pavese, G., Perrino, C., Perrone, M.G., Perrone, M.R., Putaud, J.-P., Sargolini, T., Vecchi, R., Gilardoni, S., 2014. Spatial and seasonal variability of carbonaceous aerosol across Italy. Atmos. Environ. 99, 587–598. https://doi.org/10.1016/j.atmosenv.2014.10.032.

Santiago-De La Rosa, N., González-Cardoso, G., Figueroa-Lara, J.J., Gutiérrez-Arzaluz, M., Octaviano-Villasana, C., Ramírez-Hernández, I.F., Mugica-Álvarez, V., 2018. Emission factors of atmospheric and climatic pollutants from crop residues burning. J. Air Waste Manag. Assoc. 68, 849–865. https://doi.org/10.1080/10962247.2018.1459326.

Shirmohammadi, F., Sowlat, M.H., Hasheminassab, S., Saffari, A., Ban-Weiss, G., Sioutas, C., 2017. Emission rates of particle number, mass and black carbon by the Los Angeles International Airport (LAX) and its impact on air quality in Los Angeles. Atmos. Environ. 151, 82–93. https://doi.org/10.1016/j.atmosenv.2016.12.005.

Singh, J., Payra, S., Mishra, M.K., Verma, S., 2022. An analysis of particulate pollution using urban aerosol pollution island intensity over Delhi, India. Environ. Monit. Assess. 194, 874. https://doi.org/10.1007/s10661-022-10573-z.

Styszko, K., Samek, L., Szramowiat, K., Korzeniewska, A., Kubisty, K., Rakoczy-Lelek, R., Kistler, M., Giebl, A.K., 2017. Oxidative potential of PM10 and PM2.5 collected at high air pollution site related to chemical composition: krakow case study, Air Quality Atmos. Health 10, 1123–1137. https://doi.org/10.1007/s11869-017-0499-3.

Szidat, S., Jenk, T.M., Synal, H.-A., Kalberer, M., Wacker, L., Hajdas, I., Kasper-Giebl, A., Baltensperger, U., 2006. Contributions of fossil fuel, biomass-burning, and biogenic emissions to carbonaceous aerosols in Zurich as traced by 14C. J. Geophys. Res. Atmos. 111 https://doi.org/10.1029/2005JD006590.

Turpin, B.J., Huntzicker, J.J., 1995. Identification of secondary organic aerosol episodes and quantitation of primary and secondary organic aerosol concentrations during SCAQS. Atmos. Environ. 29 (23), 3527–3544.

Vörösmarty, M., Uzu, G., Jaffrezo, J.L., Dominutti, P., Kertész, Z., Papp, E., Salma, I., 2023. Oxidative potential in rural, suburban and city centre atmospheric environments in central Europe. Atmos. Chem. Phys. 23, 14255–14269. https://doi.org/10.5194/acp-23-14255-2023.

Wedepohl, K.H., 1995. The composition of the continental crust. Geochem. Cosmochim. Acta 59, 1217–1232. https://doi.org/10.1016/0016-7037(95)00038-2.

Yu, J., Yan, C., Liu, Y., Li, X., Zhou, T., Zheng, M., 2018. Potassium: a tracer for biomass burning in beijing? Aerosol Air Qual. Res. 18, 2447–2459. https://doi.org/10.4209/aaqr.2017.11.0536.

Zanis, P., Hadjinicolaou, P., Pozzer, A., Tyrlis, E., Dafka, S., Mihalopoulos, N., Lelieveld, J., 2014. Summertime free-tropospheric ozone pool over the eastern Mediterranean/Middle East. Atmos. Chem. Phys. 14, 115–132. https://doi.org/10.5194/acp-14-115-2014.

Zhang, Q., Jiang, X., Tong, D., Davis, S.J., Zhao, H., Geng, G., Feng, T., Zheng, B., Lu, Z., Streets, D.G., Ni, R., Brauer, M., van Donkelaar, A., Martin, R.V., Huo, H., Liu, Z., Pan, D., Kan, H., Yan, Y., Lin, J., He, K., Guan, D., 2017. Transboundary health impacts of transported global air pollution and international trade. Nature 543, 705–709. https://doi.org/10.1038/nature21712.